

COMITATO NAZIONALE PER L'ENERGIA NUCLEARE
Laboratori Nazionali di Frascati

LNF - 68/66

18 Novembre 1968

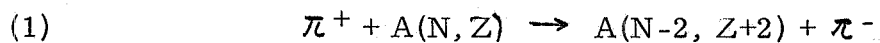
B. M. Belli, V. Di Napoli, F. Laitano, D. Margadonna, P. Picchi,
F. Salvetti and R. Visentin: DOUBLE π - PHOTOPRODUCTION
ON MEDIUM WEIGHT NUCLEI. -

Nota interna: n. 418
18 Novembre 1968

B. M. Belli^(x), V. Di Napoli⁽⁺⁾, F. Laitano^(o), D. Margadonna⁽⁺⁾, P. Picchi,
F. Salvetti⁽⁺⁾ and R. Visentin: DOUBLE π^- PHOTOPRODUCTION ON ME-
DIUM WEIGHT NUCLEI. -

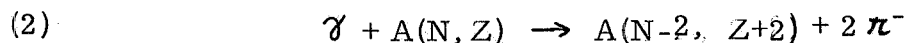
INTRODUCTION. -

Double charge exchange of pions on nuclei



can give informations on nuclear isobaric analogue states and nuclear correlations (two nucleons, at least, take part in the reaction).

We simulate the (1) (see Fig. 1) by using the beam of the electron synchrotron:



(x) - CNR

(o) - CSN- Casaccia

(+) - Istituto di Chimica dell'Università di Roma

2.

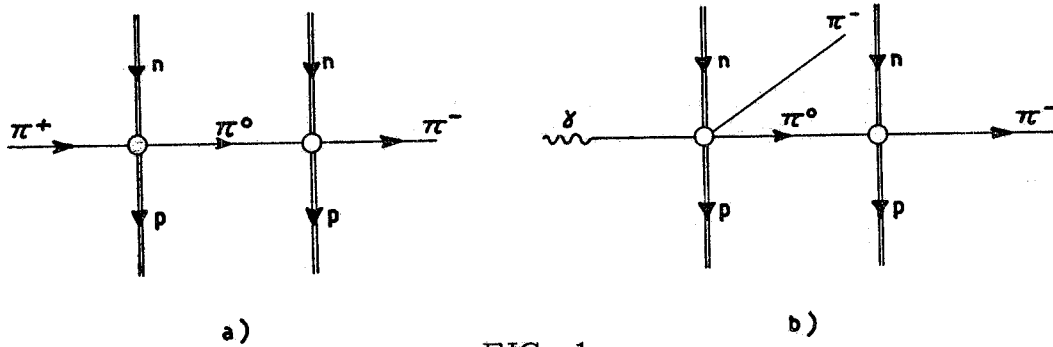


FIG. 1

The measure can be performed by detecting the γ and β radiation of A (N-2, Z+2) with coincidence methods, after the radiochemical separation have attenuate the activity of the many radionuclides formed by "spallation" reactions.

In the next paragraphs we give some remarks on the theory of the reactions (1), (2), the description of our experimental apparatus and of the radiochemical methods.

The results of the preliminary study of the reaction $\gamma + \text{Mn}^{55} \rightarrow \text{Co}^{55} + 2\pi^-$ are presented.

I. - REMARKS ON THE ISOBARIC ANALOGUE STATES OF NUCLEI. -

Many works⁽¹⁾ on proton scattering, with single isobaric analogue states ($\Delta t_z = 1$), have given much information on isospin selection rules, coulomb displacement energies, and energy level structure for a wide range of nuclear masses.

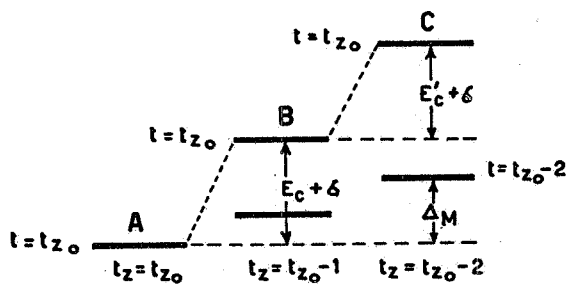


FIG. 2

These findings lead to consideration of exciting double analogue states; in Fig. 2 we show the level scheme of the three isobaric nuclei describing the transition in reaction (1) or (2). A is the target nucleus ground state. The double analogue state C lies above A by the sum of the energy increments $E_C + E'_C$ (coulomb energy) and the np mass difference.

There are measurements of E_C , and E'_C may be computed as a correction to E_C using a charged sphere model⁽²⁾;

$$E_C = \frac{6e^2}{5R} (Z + 1/2), \quad E'_C = E_C \left(\frac{Z + 3/2}{Z + 1/2} \right)$$

then

$$(3) \quad E_c + E'_c = E_c \left(1 + \frac{Z + 3/2}{Z + 1/2} \right)$$

Evaluating the (3) we obtain excitation energies which have a value of 15 ÷ 20 MeV for medium weight nuclei; they give rise to nuclear states, which could not be excited by simple mechanisms.

The wave function of the analogue⁽³⁾ state C can be written

$$\psi_C = N T_+^2 \psi_A$$

where ψ_A is the nuclear ground state, and

$$T_+ = \sum T_+(i)$$

is the isospin raising operator, N the normalization constant.

When we consider nuclei with a large neutron excess, ψ_C can represent a state obtained by a collective monopole excitation, in which pairs of neutrons have been changed into protons.

Thus the cross section of C is proportional to the neutron excess in a given shell.

The experimental situation is very little satisfactory.

The cross section for the excitation of the bound states with π meson scattering have proved to be very small. This is confirmed by the counter exp. of Gilly et al. (4) (π^- , π^0) who placed upper limits between 2×10^{-31} and 5×10^{-30} cm²/sr for reaction (1) at 200 MeV at 0° to bound states light nuclei from He⁴ to C¹².

Solomon⁽⁵⁾ and Cook and al. (6) obtained similar results: they looked in some cases specifically for the double charge exchange to states which are isobaric analogues of the ground states of the target nuclei.

However the recent activation experiments on single charge exchange reactions (π^+ , π^0 , π^- - π^0) of Allardyce et al. (7) show that the cross section is high when the overlap between initial and final wave function is large.

These experimental results seem to confirm that charge exchange reactions can give rise prevalently to analogue isobaric states, as can be predicted by the optical model.

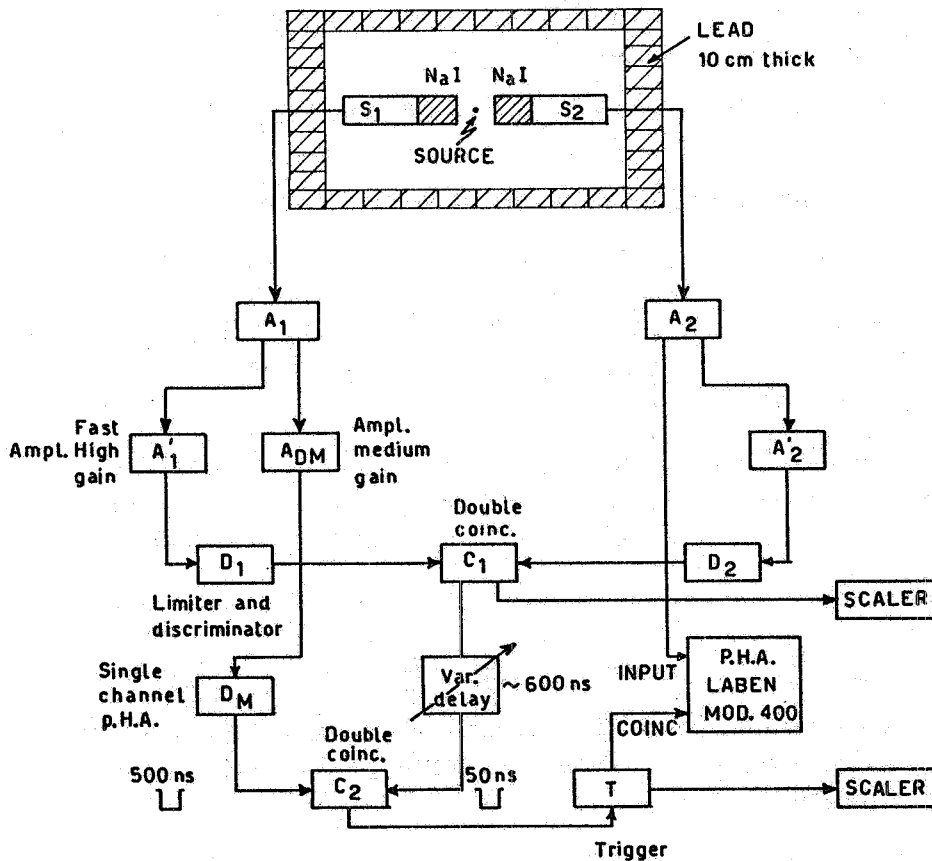
Encouraged by the results of Allardyce we think it possible to excite such states by reactions (2) and gain informations on their total cross section by measuring the activity of the A (N-2, Z+2) radionuclides.

4.

II. - THE EXPERIMENTAL APPARATUS. -

In Fig. 3 we show our experimental apparatus and the block diagram of the logic: the scintillation counters S_1 and S_2 ($3'' \times 3''$ NaI (T1)) are placed inside a cubical box ($1 \times 1 \times 1 \text{ m}^3$) whose walls are made of lead 10 cm thick. It shields the counters from cosmic rays. The radioactive source, obtained by radiochemical separation from the target irradiated by the beam, is placed between S_1 and S_2 , and their geometry is arranged to maximize the detection efficiency of the decaying products (γ radiation). The logic of Fig. 3 enable us to select a spectral line characteristic of the decaying radionuclide^(8, 9). We measure its activity by counting the events whose energy lies in the narrow peak of total absorption of the photons which correspond to the selected line. So doing we have to measure the detection efficiency of our apparatus only for the total absorption of photons of fixed energy, and we must care of its stability.

We give now a brief description of the logic.



EXPERIMENTAL APPARATUS AND LOGIC BLOCK DIAGRAM

FIG. 3

a) Coincidence C_1 .

The fast coincidence C_1 select all the events S_1, S_2 which are contemporary (in our case the master event is due to the pairs of 0.51 MeV γ rays from β^+ annihilation).

The fast discriminators D_1, D_2 shape the pulses from the counters, after they have been amplified and differenziated from the chain $A_{1,2}, A'_{1,2}$.

The resolving time τ_R of C_1 depends on the energy interval we examine and in which we must have $\eta_c = 1$ (η_c is the efficiency of the coincidence C_1 relative to the energy interval analyzed). In a rough approximation we have

$$(4) \quad \tau_R \simeq \frac{V_s \tau_s}{KA} \frac{\Delta E}{E_{\min} E_{\max}} \quad (x) \quad \Delta E = E_{\max} - E_{\min}$$

In (4) V_s is the threshold of D_1 and D_2 (V), E the energy (MeV) of the detected photons. τ_s the rise time of the pulses from S_1, S_2 (a typical value of τ_s for $N_aI(Tl)$ chrystals is ~ 450 ns). A the total amplification of the chain $A_{1,2}, A'_{1,2}$, K (Volt/MeV) the conversion coefficient "energy lost in the chrystal amplitude" of the pulse at the photomultiplier^(o) anode.

τ_R measures the maximum time jitter of the pulses at the output of D_1 and D_2 (see Fig. 4).

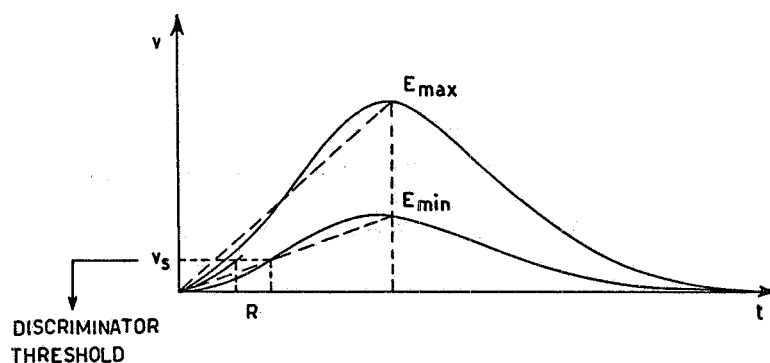


FIG. 4

(x) - We have approximated the rise time of the pulse from NaI counter with a linear ramp from zero level to its maximum.

(o) - As is well known the maximum amplitude of the pulse from NaI counters is linearly related to the energy lost by the γ in the chrystal.

6.

In our case $K = 10^{-1}$ Volt/MeV, $V_g = 0.3$ Volt, $A \sim 600$. The energy interval to which the main spectral lines of our radionuclides belong is about 2 MeV ($E_{\min} = 0.05$ MeV, $E_{\max} = 2.05$ MeV). From these condition we have $\tau_R \sim 50$ ns, which is the resolving time of C_1 .

b) Coincidence C_2 .

The coincidence C_2 selects among the events of C_1 all those in which $V_{S1} = V_M \pm \Delta V_M$ ($E_M \pm \Delta E_M$). We have fixed the amplitude V_M by the single channel analyzer D_M . Our choice of V_M corresponds to an energy $E_M = .51$ MeV, $\Delta E_M = .075$ MeV, being E_M the energy of a photon from β^+ annihilation and $2\Delta E_M$ the total width of the 0.51 MeV absorption photopeak in our counters.

The output from C_2 enables the pulse height analysis on S_2 by means of the multichannel analyzer.

So doing the amplitude spectrum of S_2 give us all the spectral lines, which our apparatus can resolve, of the decaying source (as an example if N^{22} is placed between S_1 S_2 we obtain three lines corresponding to 0.51 MeV (β^+ annihilation), 1.27 MeV (deexcitation γ), 1.78 MeV (sum energy of the 0.51 ± 1.27 quanta).

We have paid particular attention to the chain A_1, A_{DM}, D_M . Its stability give us a constant detection efficiency of the amplitudes of S_1 (near the .51 MeV photopeak), hence a constant efficiency for all the lines in the amplitude spectrum of S_2 . Fig. 5 shows the response of the chain $A_1 \rightarrow A_{DM} \rightarrow D_M$.

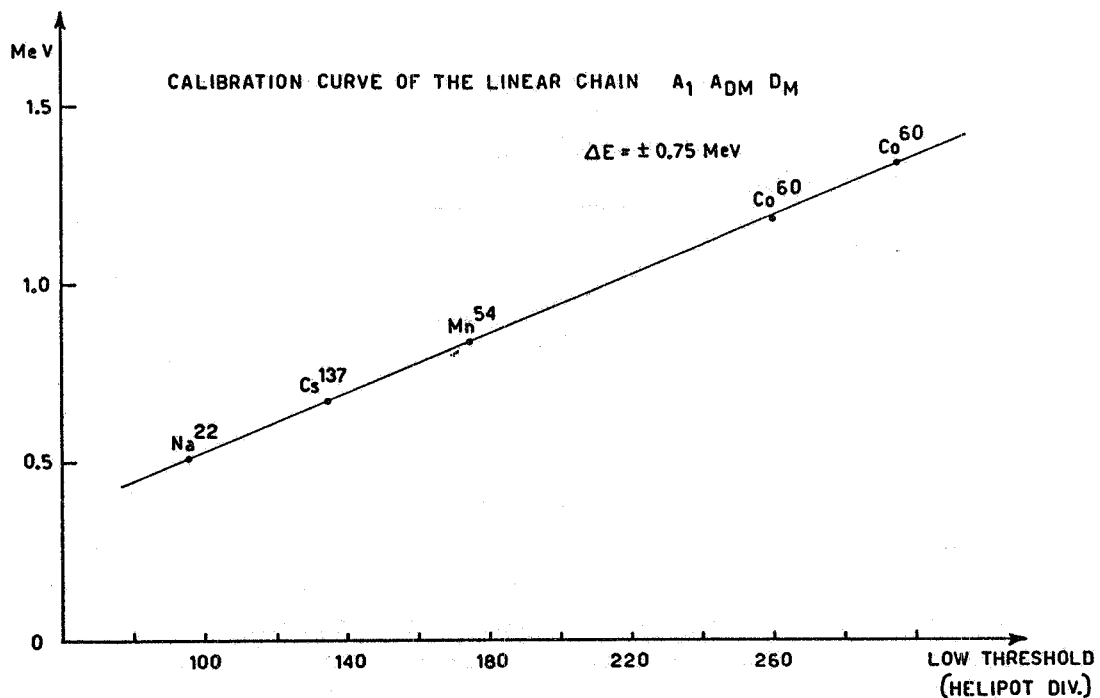


FIG. 5

c) The reaction $\gamma + {}^{55}_{25}\text{Mn} \rightarrow {}^{55}_{27}\text{Co} + 2\pi^-$.

As a first example of (2) we have begun to study the reaction

$$\gamma + {}^{55}_{25}\text{Mn} \rightarrow {}^{55}_{27}\text{Co} + 2\pi^-$$

${}^{55}_{25}\text{Mn}$ is a medium weight nucleus with a 5 neutrons excess. So it should be rather favoured for the transition.

${}^{55}_{27}\text{Co}$ is an unstable nuclide (half life $T_{1/2} = 18.2$ h). The decay scheme ${}^{55}_{27}\text{Co}$ is shown in Fig. 6.

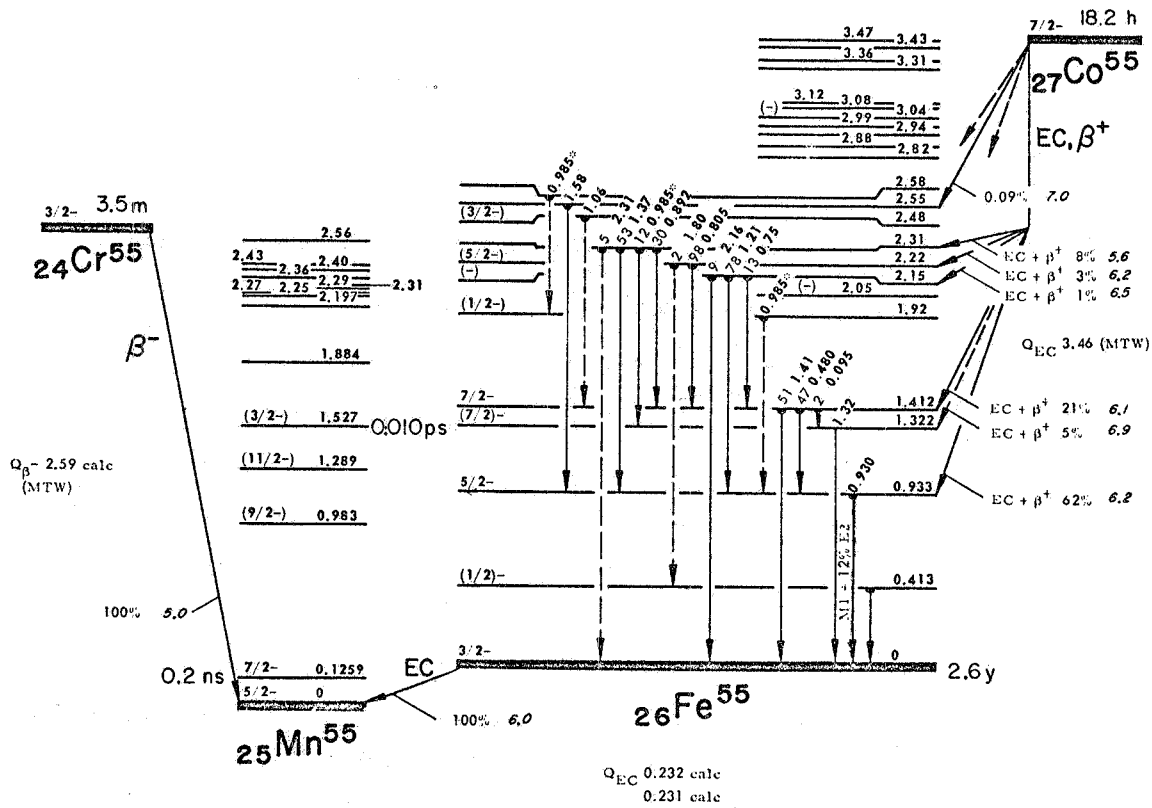


FIG. 6

As we see a good channel for our coincidences is represented by the β^+ decay; which gives a pair of collinear .51 MeV photons.

So the activity measurements were performed on the events of the .51 MeV total absorption peak.

In our measure we could not resolve unambiguously the .93 MeV line because of the poor statistics of our events (due to the low cross section and the short exposures we could execute), the relatively high background in our apparatus (~ 20 events/h in the .51 MeV peak, and of the same order in the .93 peak, due essentially to cosmic rays and to natural

8.

radioactivity of the lead shield), and the relative low detection efficiency of the NaI crystals for .93 MeV photons (in our apparatus we measured $\frac{\eta(.93 \times .51)}{\eta(.51 \times .51)} \approx 7 \times 10^{-2}$, being η the whole detection efficiency of our coincidence system)^(x).

The .47 MeV line is not resolved by NaI crystals from the (more intense) .51 MeV line. These lines can be separated by using solid state detectors, but their efficiency for γ rays is too and they could'nt be used when low activity measurements are performed⁽¹⁰⁾.

To the .51 MeV channel contribute many other unstable nuclides formed by spallation reactions, and their high activity obscure the one of $^{55}\text{Co}_{27}$.

In Table I are the most important of them:

TABLE I

	reaction	T 1/2	decay	Total cross section cm ²
$^{52}_{25}\text{Mn}$	$\gamma, 3n$	5,7 d	$\beta^+, 0,6, K^{(o)}$	5×10^{-28}
$^{48}_{23}\text{V}$	$\gamma, 2p, 5n$	16,2 d	$\beta^+, 0,7, K$	1.2×10^{-28}
$^{52}_{26}\text{Fe}$	$\gamma, 3n, -$	8 h	$\beta^+, 0,8, K$	5×10^{-29}

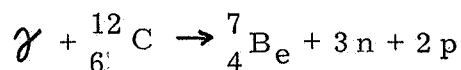
Thus our activity measurements on ^{55}Co can be performed only if this nuclide can be separated from all the other unstable nuclides in the irradiated ^{55}Mn target. This is done by radiochemical methods.

d) The radiochemical separation. -

The $^{55}_{25}\text{Mn}$, powdered and packaged with a thin polietilene disk, is exposed to the γ beam of the electronsynchrotron (see Fig. 7). We used the polietilene disk as a monitor of our beam; the total equivalent quanta, absorbed by the target, were obtained by measuring the activity of the ^7_4Be formed in the reaction

(x) - $\eta(.93 \times .51)$ is the efficiency of the coincidence for two γ rays of energy .93 MeV and .51 MeV respectively.

(o) - K = electron capture



of which the total cross section have been measured⁽¹¹⁾.

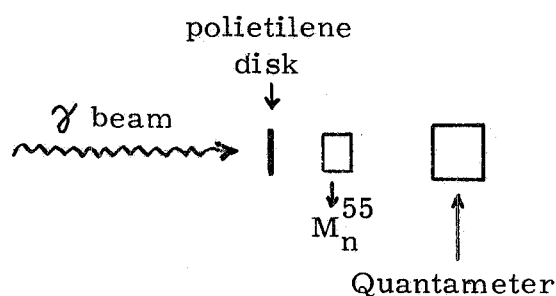


FIG. 7

The irradiated Mn (about 2 g) was dissolved in 6 M HCl. Carrier solutions of each cation Co(II), Fe(II), Fe(III), Cr(III), Sc(III), Ti(III) in the form of chlorides were added. In the case of vanadium, NaVO_3 was added.

In each case, except Co(II) (100 mg), 50 mg of the cation were used.

The mixture was processed according to the procedure outlined below and the final precipitate was weighed before counting. The chemical yield of cobalt was calculated by determining the weight of precipitate obtained from the amount of carrier added.

Fe, Sc, Ti, Cr and V were precipitated in the form of hydroxides, adding 2 g of NH_4Cl and enough NH_4OH to reach a pH = 6.8. The precipitates were separated from the solution by means of a centrifuge.

Carriers of Na(I), K(I) and Mg(II) (50 mg of each cation) were added to the supernatant and the mixture was treated by H_2S . After centrifugation, the precipitate of CoS , with (small amounts) of MnS , was washed several times by a solution of 0.1 M HCl and was dissolved again by means of 14 M HNO_3 .

The cobalt solution was opportunely treated by KOH so that a pH=6 was obtained. Carrier solutions of Mn(II) and Fe(II) (50 mg) in the form of acetates were added.

$\text{K}_3\text{Co}(\text{NO}_2)_6$ was heat precipitated by adding solid KNO_2 and then cooled at 0°C . The precipitate was separated from the solution by means of a centrifuge and was washed a first time by a 6% KNO_2 solution, a second time by $\text{C}_2\text{H}_5\text{OH}$ and at last by $(\text{C}_2\text{H}_5)_2\text{O}$.

The cobalt precipitate was dried for ten minutes at 110°C and weighed in the form of $\text{K}_3\text{Co}(\text{NO}_2)_6 \cdot \text{H}_2\text{O}$.

In the case of a double separation, the cobalt precipitate so obtained, was heat dissolved by 5. M. H_2SO_4 . Carriers of Fe(III), Mn(II), Cr(III), V(V), Ti(III) and Sc(III) (50 mg of each cation) were added to our solution and the chemical separation was carried out again as we said above.

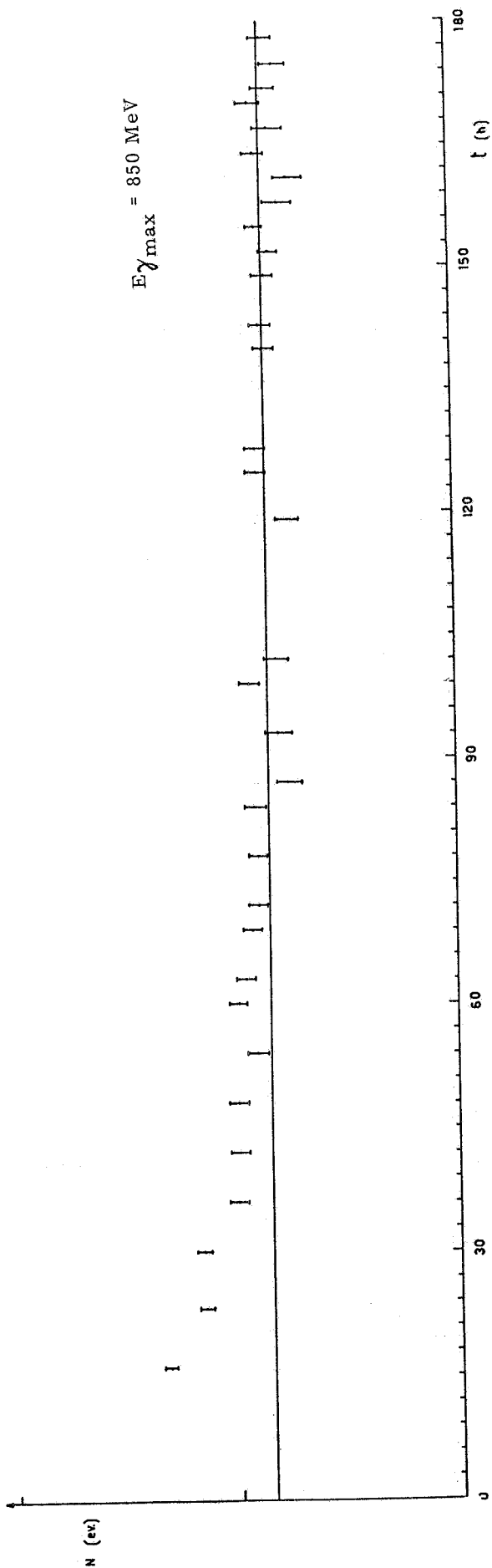


FIG. 8

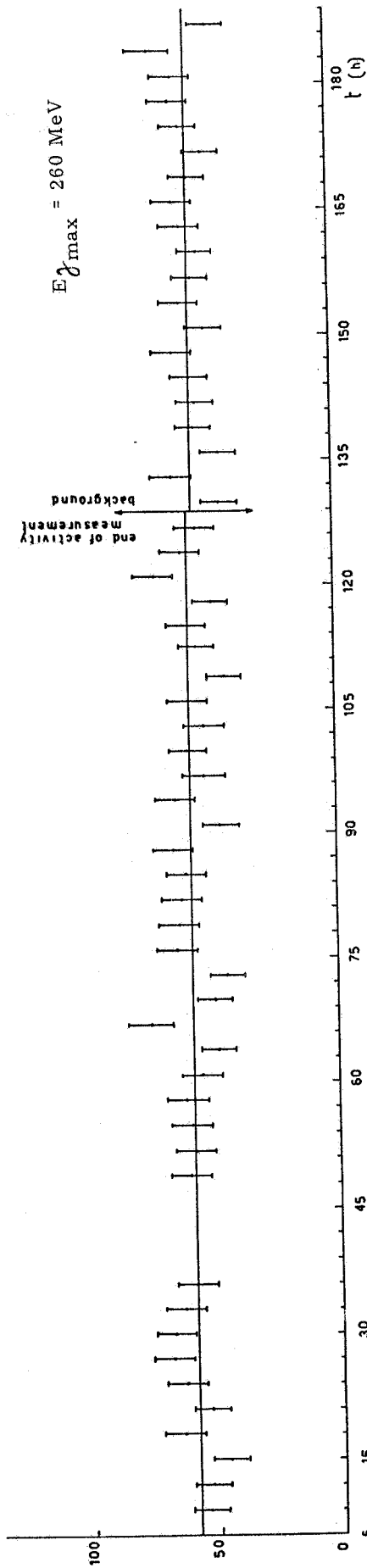


FIG. 9

III. - RESULTS AND ANALYSIS. -

We have made two exposures of the ^{55}Mn target to the γ beam, the maximum energy $E_{\gamma\text{max}}$ was:

a) 850 MeV, well above and b) 260 MeV, well below the double pion photoproduction threshold on nucleon.

Fig. 8, 9 show the results of the activity measurements. In the 260 MeV run (see Fig. 8) we measured a very low activity with a long half life, while the data of Fig. 9 (850 MeV) show a short half life component together with a long half life one.

By subtracting this background activity we obtain the distribution of Fig. 10 for the short half life events.

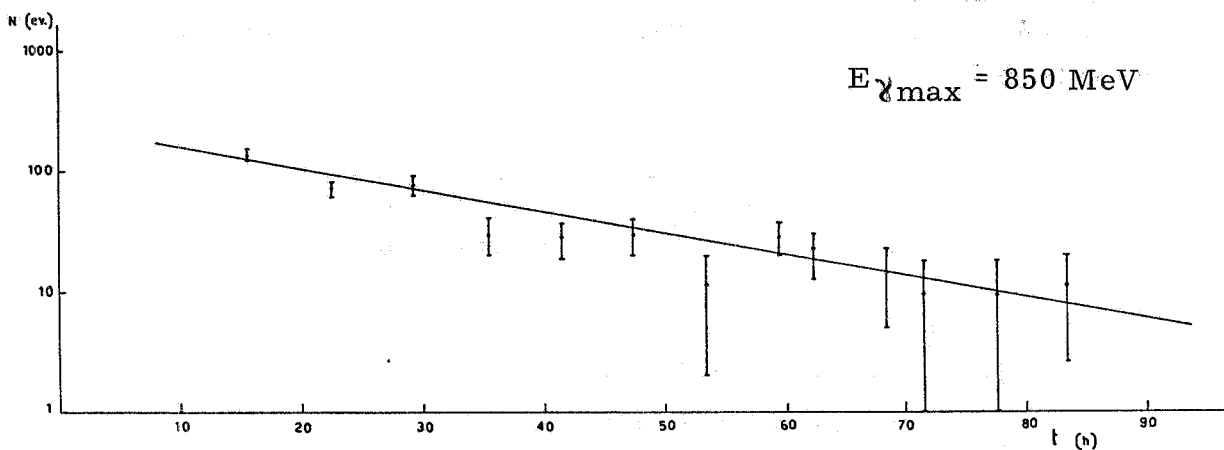


FIG. 10

A best fit of this points with an exponential function:

$$(5) \quad \log A = C - \lambda t$$

(being A the activity, $1/\lambda = \tau$ decay constant) gives $C = 5.38 \pm .14$ and $\lambda = 1/T = 3.96 \times 10^{-2} \pm .0045 \text{ h}^{-1}$ (6). We think that our events can be attributed to Co^{55} for the following reasons:

a) the decay constant $\tau = 1/\lambda = 25\text{h}$ is in the range of values defined by (6).

b) We have not measured any short half life activity near $T_{1/2} = 18\text{h}$ below the double pion photoproduction threshold.

c) The short half life component ($T_{1/2} = 18\text{h}$) was present also in a sampling on which a double cycle of radiochemical separation has been made.

The mean cross section of (2) in the energy interval $E_{\gamma\text{thresh.}}$ $E_{\gamma\text{max}}$ is

12.

$$(7) \quad \langle \sigma \rangle = \frac{A_1}{N_{f_c} \Delta x} \frac{A_p}{N_p}$$

where A_1 is the extrapolated activity to the instant at which end the exposure. By taking in account (5) we have

$$(8) \quad A_1 = \frac{e^c}{\int_0^{t^x} e^{(t-t^x)/\tau} dt (1 - e^{-1/\tau}) E_{f_s} R \epsilon_\omega E_c}$$

t^x is the time interval (h) of the exposure (and we consider the mean intensity of the beam in this time interval), E_{f_s} is the efficiency of the radiochemical separation ($E_{f_s} \approx .7$), E_c the total efficiency of our apparatus measured at the .51 MeV total absorption peak ($E_c \approx .9$), $R = .8$ is the ratio of the mode of decaying of Co^{55} we have considered to the total modes, $\epsilon_\omega = \Delta\omega/4\pi \approx 1$ the solid angle efficiency (our counters covers practically all the solid angle).

$$(9) \quad N_{f_c} = \frac{N_D K_Q F}{E_{\gamma_{max}} t^x} \int_{E_{thresh}=320}^{E_{\gamma_{max}}} \frac{1}{E} dE$$

In (9)

N_D = total number of doses

K_Q = quantameter constant

F = conversion factor farad coulomb

A_p = 55 atomic weight of Mn_{25}^{55}

N_p = Avogadro number

ρ = 7.2 gr/cm³ Mn^{55} density

Thus the mean cross section in the energy interval 320-850 MeV we measure is

$$\langle \sigma \rangle = (2.1 \pm .8) 10^{-32} \text{ cm}^2$$

ACKNOWLEDGMENTS. -

The authors wish to thank Prof. P. E. Argan who suggested this measure and participated to its early stages.

REFERENCES. -

- (1) - J. Fox and D. Robson (eds.) Isobaric-spin in nuclear phys. (Academic Press, New York, 1966).
- (2) - C. J. Batty, E. Friedman and P. C. Rowe, Phys. Letters 19, 33 (1965).
- (3) - G. E. B. Rown and S. Barshay, Phys. Letters 16, 165 (1965).
- (4) - L. Gilly et al. , Phys. Letters 19, 335 (1965).
- (5) - J. Solomon, Proc. Conf. on Intermediate Energy Physics (Williamsburg 1966), Vol. 1, p. 269.
- (6) - C. J. Cook, R. L. Burman and M. E. Nordberg, Bull. Am. Phys. Soc. 12, 104 (1967).
- (7) - B. W. Allardyce, D. T. Chivers, J. J. Domingo, E. M. Rimmer, N. W. Tanner and R. C. Whitcomb, Phys. Letters 26, 573 (1968).
- (8) - K. Siegbahn, Alpha, Beta and γ ray spectroscopy (North Holland Publishing Company, Amsterdam, 1965).
- (9) - S. Tanaka, R. Sakamoto and J. Takagi, Nuclear Instr. and Meth. 56, 319 (1967).
- (10) - J. M. Hollander, Nuclear Instr. and Meth. 43, 65 (1966).
- (11) - V. DiNapoli, F. Dobici, O. Forina, F. Salvetti and H. G. De Carvalho, Nuovo Cimento 55B, 95 (1968).